

Seafloor Ripple Measurements at the Martha's Vineyard Coastal Observatory

Alex E. Hay
Dalhousie University
Department of Oceanography
Halifax, N.S.
Canada B3H 4J1

Phone: (902) 494-6657 Fax: (902) 494-2885 Email: alex.hay@dal.ca

Grant Number: N00014-04-1-0647

http://www.phys.ocean.dal.ca/people/po/Hay_Alex.html

LONG-TERM GOAL

The long-term goal is to quantify ripple and ripple field properties in response to wave and current hydrodynamic forcing and grain size variability.

OBJECTIVES

The overall objective of the 2007 experiment at the Martha's Vineyard Coastal Observatory (MVCO) is to investigate the relative adjustment of ripples in the coarse and fine sands to forcing events involving a range of different surface gravity wave and mean current forcing conditions, as a function of cross-shore distance (i.e. water depth).

Our primary objective is to determine the temporal and spatial evolution of wave-forced seafloor ripple geometry and as a function of both hydrodynamic forcing (as modulated by water depth) and grain size (fine and coarse sand).

The observations will be used to validate existing models and to develop new models for ripple geometry as a function of forcing hydrodynamics and seabed characteristics. The observations will also have a smaller focus on small scale sediment transport processes over ripples and larger scale wave field variability over spatially variable ripples. The small scale sediment transport process observations, which combined with realistic transport – morphodynamic models being developed by other investigators, will lead to physics-based models of ripple evolution.

Wave models, initiated with the measured wave directional spectrum offshore, will be used to generate predicted wave fields for comparison to co-located observations of wave and ripple properties across the shoaling region, in both fine and coarse sand. These results will provide the basis for extending ripple property predictions based on the modeled waves to the full experimental domain. These predictions will be tested against the sidescan/multibeam survey data.

APPROACH

The above objectives are being carried out in collaboration with Dr. Peter Traykovski (Woods Hole Oceanographic Institution), Dr. Tom Herbers (Naval Postgraduate School), and Dr. Chris Sherwood (US Geological Survey). The MVCO site is characterized by longshore-alternating tongues of coarse

Report Documentation Page

Form Approved
OMB No. 0704-0188

Public reporting burden for the collection of information is estimated to average 1 hour per response, including the time for reviewing instructions, searching existing data sources, gathering and maintaining the data needed, and completing and reviewing the collection of information. Send comments regarding this burden estimate or any other aspect of this collection of information, including suggestions for reducing this burden, to Washington Headquarters Services, Directorate for Information Operations and Reports, 1215 Jefferson Davis Highway, Suite 1204, Arlington VA 22202-4302. Respondents should be aware that notwithstanding any other provision of law, no person shall be subject to a penalty for failing to comply with a collection of information if it does not display a currently valid OMB control number.

1. REPORT DATE 2007		2. REPORT TYPE		3. DATES COVERED 00-00-2007 to 00-00-2007	
4. TITLE AND SUBTITLE Seafloor Ripple Measurements at the Martha's Vineyard Coastal Observatory				5a. CONTRACT NUMBER	
				5b. GRANT NUMBER	
				5c. PROGRAM ELEMENT NUMBER	
6. AUTHOR(S)				5d. PROJECT NUMBER	
				5e. TASK NUMBER	
				5f. WORK UNIT NUMBER	
7. PERFORMING ORGANIZATION NAME(S) AND ADDRESS(ES) Dalhousie University, Department of Oceanography, Halifax, N.S., Canada B3H 4J1,				8. PERFORMING ORGANIZATION REPORT NUMBER	
9. SPONSORING/MONITORING AGENCY NAME(S) AND ADDRESS(ES)				10. SPONSOR/MONITOR'S ACRONYM(S)	
				11. SPONSOR/MONITOR'S REPORT NUMBER(S)	
12. DISTRIBUTION/AVAILABILITY STATEMENT Approved for public release; distribution unlimited					
13. SUPPLEMENTARY NOTES					
14. ABSTRACT					
15. SUBJECT TERMS					
16. SECURITY CLASSIFICATION OF:			17. LIMITATION OF ABSTRACT	18. NUMBER OF PAGES	19a. NAME OF RESPONSIBLE PERSON
a. REPORT unclassified	b. ABSTRACT unclassified	c. THIS PAGE unclassified			

and fine sand, varying in width from O(100 m) to O(1 km), extending several km in the cross-shore direction. The overall plan for the experiment was to deploy an array of high-resolution rotary sonars a suite of flow and wave measurements, and to conduct sediment sampling and sidescan/multibeam surveys.

My contribution to the field program was to deploy 4 instrumented bottom pods, each equipped with rotary sonars to measure ripple properties (spatial pattern, height, wavelength, orientation, etc.) and sensors to measure the local flow conditions (mean currents, wave orbital velocities and pressure, wave directional spectra). The four pods were deployed in adjacent tongues of coarse and fine sand, at 12-m and 16-m water depths. Three of the pods were cabled to the observatory nodes, providing continuous power and real-time communications. The fourth site was too far from the closest node to be cabled, and was thus autonomous. To provide redundancy and (in the case of the rotary sonars) increased spatial coverage, duplicate sensors were mounted on the cabled pods. (Battery and instrumentation limitations precluded the use of redundant sensors on the autonomous pod.)

There were several technical “firsts” (for us) that were required for this experiment. In previous experiments (SAX04, SandyDuck, etc.), I had always operated in cabled mode. Thus, the autonomous capability was new, and had to be developed. Also, our rotary sonars are analog, and previously had to be cabled individually to a shore- or ship-based controller. We developed the hardware and software needed to implement this function *in situ*, enabling each connected pod to operate via a single cable using Ethernet protocol.

We monitored and controlled the operation of the cabled pods via the Internet. This allowed us to alter data acquisition protocols, to watch data files being opened and closed in real time, and to monitor any errors (e.g. a communications failure to an instrument), also in real time, via a JAVA-based GUI. Depending upon the nature of the error, we then stopped acquisition to take appropriate action. These “fixes” involved: (1) modifying the sensor configuration parameters; (2) modifying the data acquisition code to fix a previously unidentified bug; or (3) in one instance a hard reboot (power cycle) of the system. After some initial teething problems in following the deployment of the instruments in late August resulting in the loss of a few of the hourly data files, the system operated flawlessly since mid-September.

Except when trouble-shooting, we could not monitor the data in real-time because of the limited bandwidth of the T1 connection to the Vineyard. Block data transfers to Dalhousie occurred on an hourly basis. A daily check of data files from individual sensors was maintained as a quality control measure and to identify any significant changes in ripple geometry which might prompt Peter Traykovski to carry out a REMUS survey.

WORK COMPLETED

Except for one rotary fan beam sonar on the cabled pod at 16-m depth, the data return from the (13!) remaining rotary sonars was 100%. (Note that because 2 fan beam sonars were mounted on each cabled pod, the loss of this one sonar will not impact the data set significantly.) Similarly, almost all of the flowmeters appear on the basis of the data analyses to date to have functioned well, and to have produced high quality data particularly during active transport conditions. (Some of the single-point acoustic Doppler velocimeters produced noisy data during quiescent conditions, presumably due to scatterer concentrations being low at these times.) Given that this was a first-time field deployment of our autonomous pod, and of the data acquisition and control (DAQ) interface for the analog rotary

sonars, it is especially gratifying that both the autopod and the DAQ interfaces for the 4 rotary sonars on each cabled pod functioned flawlessly throughout the course of the 2-month experiment.

At this point in time, two weeks after the completion of the experiment, we have examined the data from all of the sensors. Level 1 quality-assured data products have been generated for the flowmeters for the complete experiment. The rotary sonar data have been processed from all of the connected pods for the first and last storm events. The processing of the autopod sonar data for these events is underway.

RESULTS

Figure 1 shows time series of significant wave height, determined from the flowmeters on each of the 3 cabled pods using linear wave theory. Note the high level of coherence between the data from different sensors. Note also the close correspondence between wave heights derived from velocity, and those from pressure. Both comparisons give confidence in the quality of the data. Note as well the very similar wave heights in 12- and 16-m depth, suggesting that shoaling, refraction and dissipation effects between 16 m and 12 m were not very large for these events. Preliminary simulations using the Simulating Waves Nearshore (SWAN) model tend to support this conclusion.

Figures 2 and 3 show example rotary sonar images of the seabed at the coarse and fine sand sites in 12-m depth, before and after the forcing event in mid-September (YD254-256). Focussing initially on the long-wavelength (ca. 70-cm) ripples in coarse sand, marked changes are indicated: from the degraded, relict ripples in the first image, to the fresh, sharp-crested ripples in the second. Note also the change in the orientation of the long-wavelength ripples in the two images. In contrast, the ripples in the fine sand (Figure 3) are much shorter (ca. 20-cm wavelength), and the sharp acoustic shadows in the first image indicate that these ripples are active. Indeed, comparing this image with the first coarse sand image in Figure 2, one can see that the short ripples on the crests of the long-wavelength ripples have the same orientation as the ripples in the first image in Figure 2. The post-storm ripple pattern in Figure 3 is roughly similar to the pre-storm pattern, though somewhat more irregular.

Figure 4 shows the sea-swell band wave energy and direction. Note the high coherence among the measurements at the different locations, another indicator of data quality. Figure 5 shows the ripple crest orientations: that is, the angle of the normal to the ripple crests, in the same coordinate system as the wave directions in Figure 4. There is satisfying agreement between the ripple orientations at the two fine sand sites, and for both fanbeam sonars at FS12, before and after the two forcing events. At the 12-m coarse sand site, there is a 5-10 degree offset between the orientations from the two fanbeam sonars: as explained in the caption, the signals from one of these sonars (FANa) was relatively weak, so the seabed images are not as clear at larger ranges, possibly resulting in the offset.

It is immediately obvious that the evolution of ripple orientation during forcing events is captured in these data for coarse sand, but not in fine sand, an exception being the 2nd weaker forcing event (on YD297) at FS16. This is because, for sufficiently energetic conditions, the bed state in fine sand undergoes transition from 2-d orbital scale ripples to non-orbital scale, 3-dimensional ripples and even nearly flat bed. During these periods, anorbital short wavelength ripples are often present, however, and so there is potential that with further processing ripple orientations can be extracted during these periods.

This possibility (i.e. that anorbital ripple orientations can be tracked in fine sand during the course of a storm) is illustrated in Figure 6a through c, for the YD293-294 forcing event, at sites FS12 and FS16. The red data points are the orientations determined from the high spatial frequency band (5 to 30 cpm), corresponding to anorbital ripples. It is clear from these figures that high-pass filtering does indeed help to fill the gap (compare Figures 5 and 6). The anorbital ripple orientations are somewhat noisy, however, and the estimates really do not settle down until the waning stages of the storm.

The question of when ripple adjustment in fine versus coarse sand stops as the forcing diminishes was one of the principal motivating questions behind this experiment. Figure 6d shows the orientation time series at CS12 during the YD293-294 event, while Figure 6e and 6f show the incident wave direction and energy at the three sites. The main point indicated by these results is that, whereas the ripple orientations in coarse sand at the end of the storm are ca. -10 degrees, those in fine sand are ca. -20 degrees, and that this 10-degree difference in ripple crest orientation can be understood in terms of the differences in wave direction at the thresholds of sediment motion for the two sand sizes. The wave energies and directions at the threshold of motion are indicated by the vertical blue lines in Figure 6d and e, and have been transposed to Figures 6a through d as appropriate.

In summary, the analyses-to-date of the records from the MVCO ripples experiment indicate that we have obtained a high quality data set. In particular, the high coherence among the flowmeter measurements, and their consistency with linear theory and with the SWAN model predictions, indicate that the results for the forcing are reliable. The time series of seabed images obtained with the rotary sonars provides is complete, providing continuous information on the ripple patterns and amplitudes at the four sites. The ripple orientation estimates presented here, while a work in progress especially for periods of active adjustment, are promising nonetheless, especially in relation to the central question of the experiment: grain-size dependent differences in ripple evolution.

PUBLICATIONS

Hay, A.E., 2007, Near-bed turbulence and relict wave-formed sand ripples: Observations from the inner shelf, *J. Geophys. Res.* [in press, refereed].

Newgard, J.P. and A.E. Hay, 2007. Turbulence intensity in the wave boundary layer and bottom friction under (mainly) flat bed conditions, *J. Geophys. Res.*, 112, C09024, doi:10.1029/2006JC003881 [published, refereed].

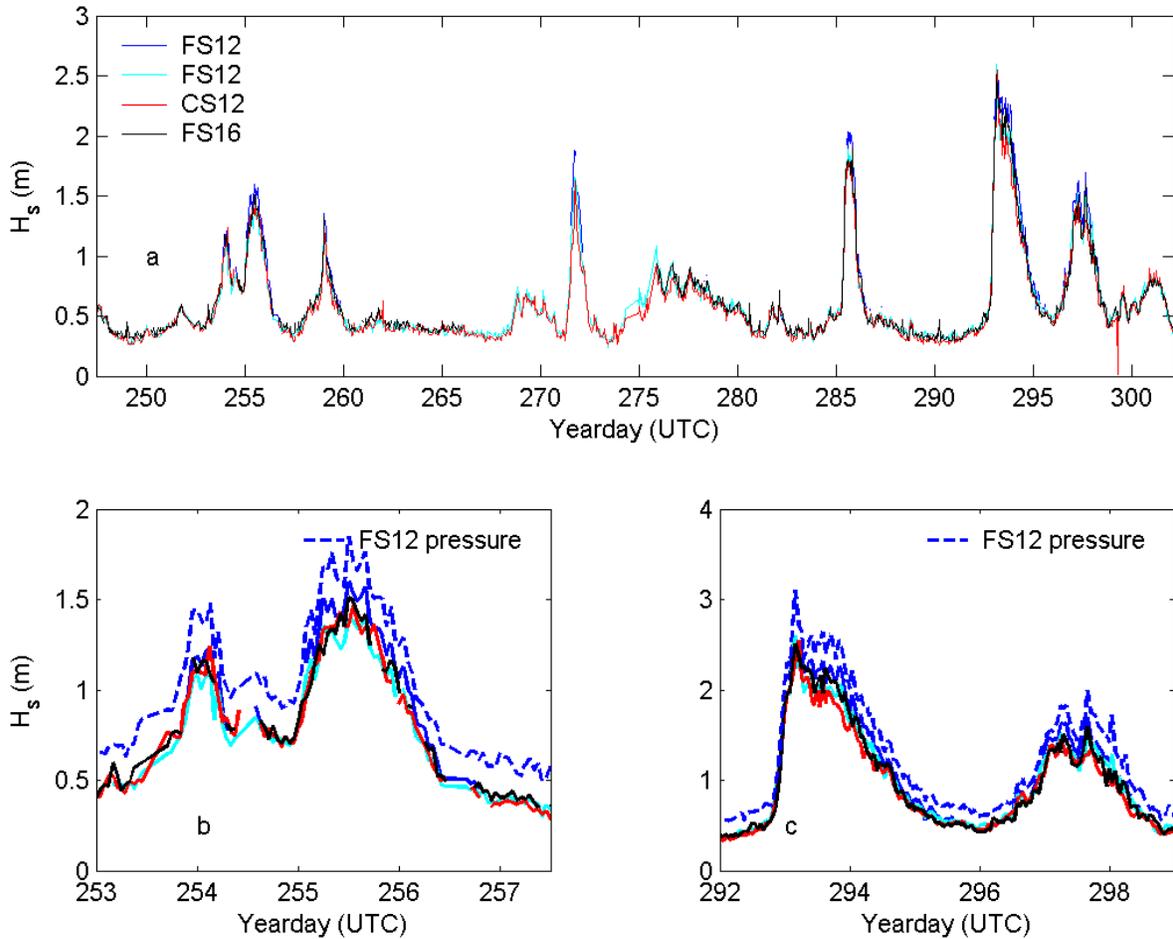


Figure 1. Significant wave height time series, determined from the flowmeter measurements assuming linear wave theory. (a) Representative time series from the flowmeters, for the full experiment (a), and the first (b) and last(c) storm events, at sites FS12 (fine sand, 12 m), CS12 (coarse sand, 12 m), FS16 (fine sand, 16 m). The solid lines are derived from velocity. The dashed blue line in b and c is derived from pressure, and is offset in the vertical by 0.1 m.

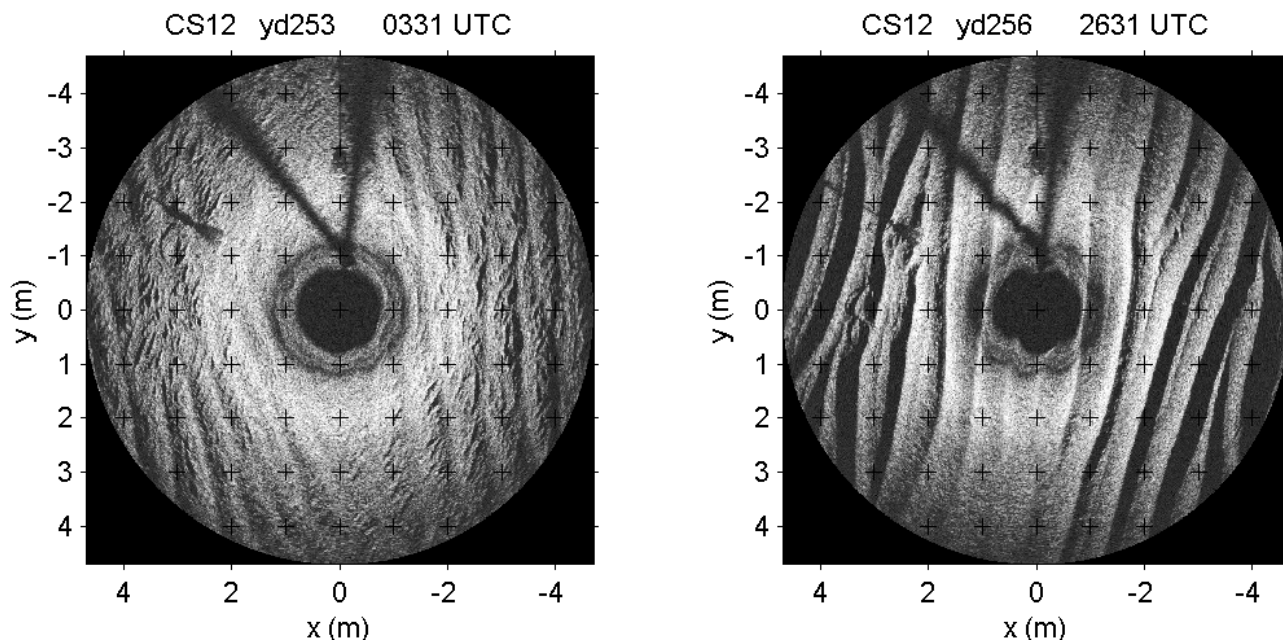


Figure 2. Rotary fanbeam (i.e. sidescan) images of the seabed at CS12, the coarse sand site in 12-m water depth, before and after the forcing event in mid-September. The x-direction is approximately shorenormal, and positive shoreward.

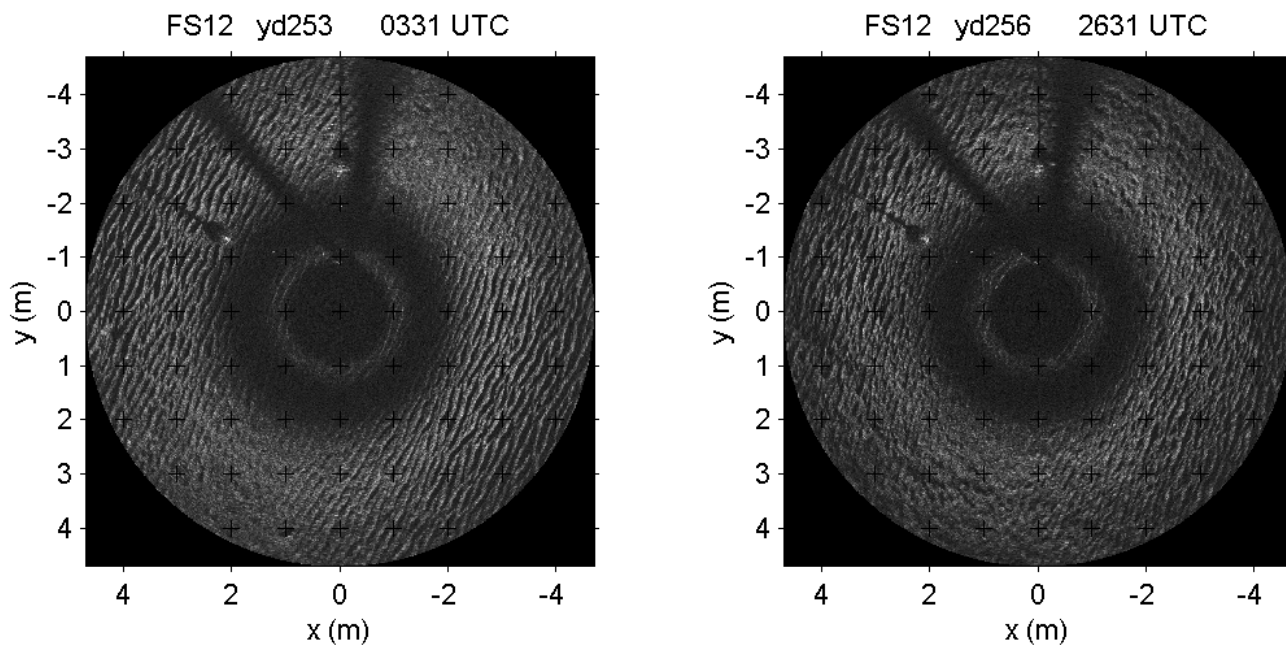


Figure 3. As in Figure 1, but at FS12, the fine sand site in 12-m depth.

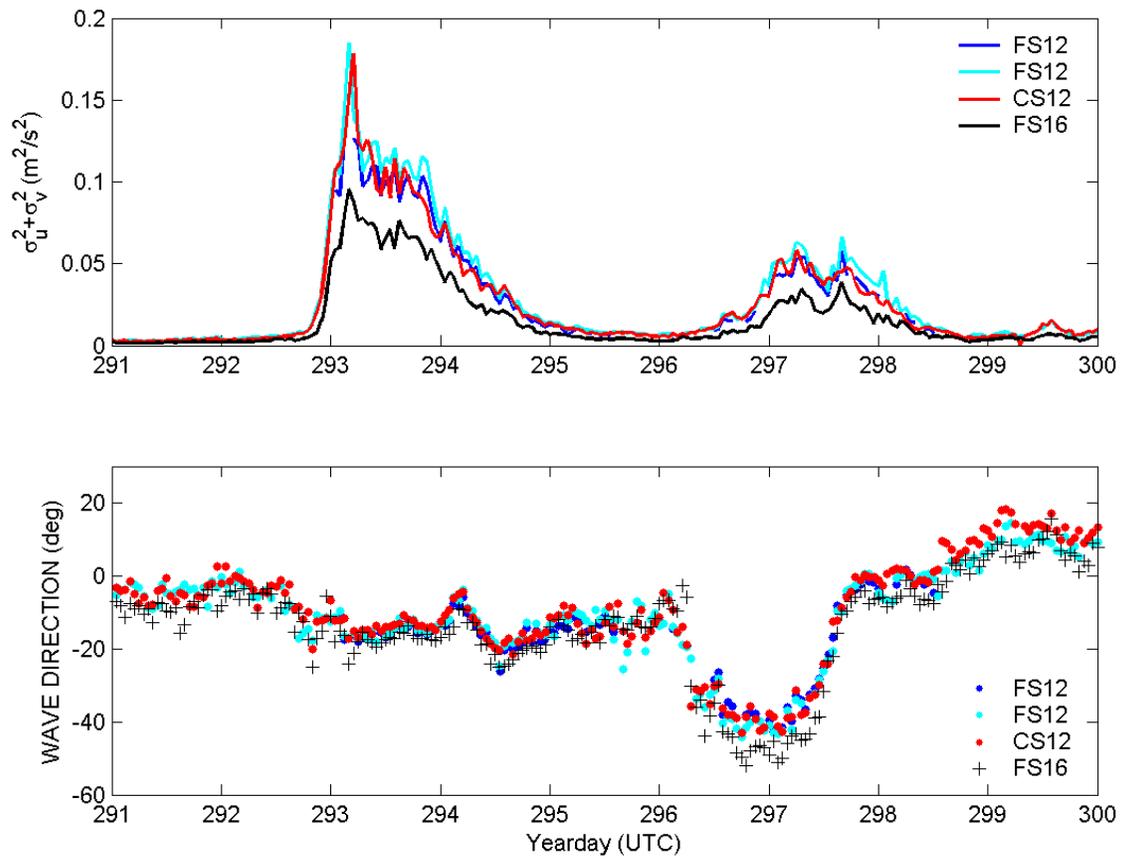


Figure 4. Time series of: top panel, kinetic energy in the sea-swell band at the three cabled pods; bottom panel, wave direction (to, 0-degrees being approximately shore normal, relative to magnetic north)).

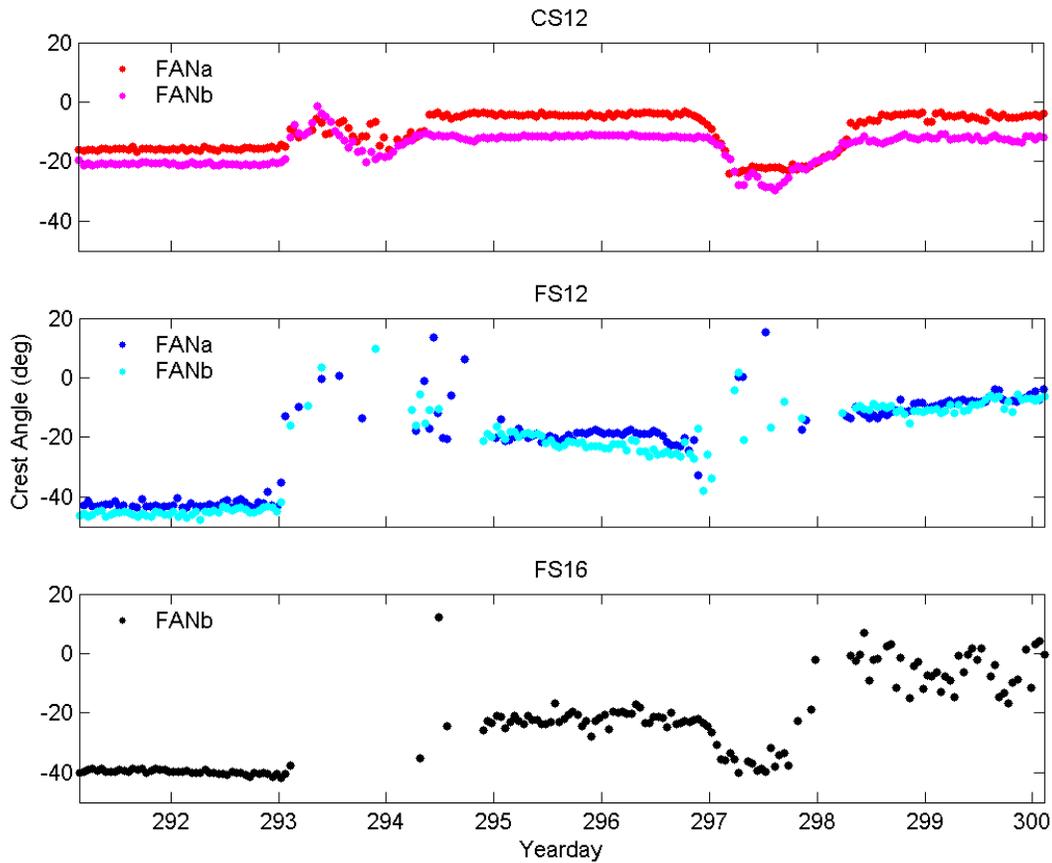


Figure 5. Ripple orientation during the final storm event, the same period as the wave directions in Figure 4. The gaps in the FS16 record and the “noise” in the FS12 record on YD293-294, and YD297, correspond to 3-dimensional or nearly flat bed states during high wave energy (Figure 4). The 5-10 degree offset between the results for the 2 fanbeams at CS12 are an artifact of the weaker signals for FANa at that site: the FANb results are more reliable. Note the correspondence between the trends in these ripple crest orientations and the wave directions in Figure 4, especially for CS12 and FS16 sites.

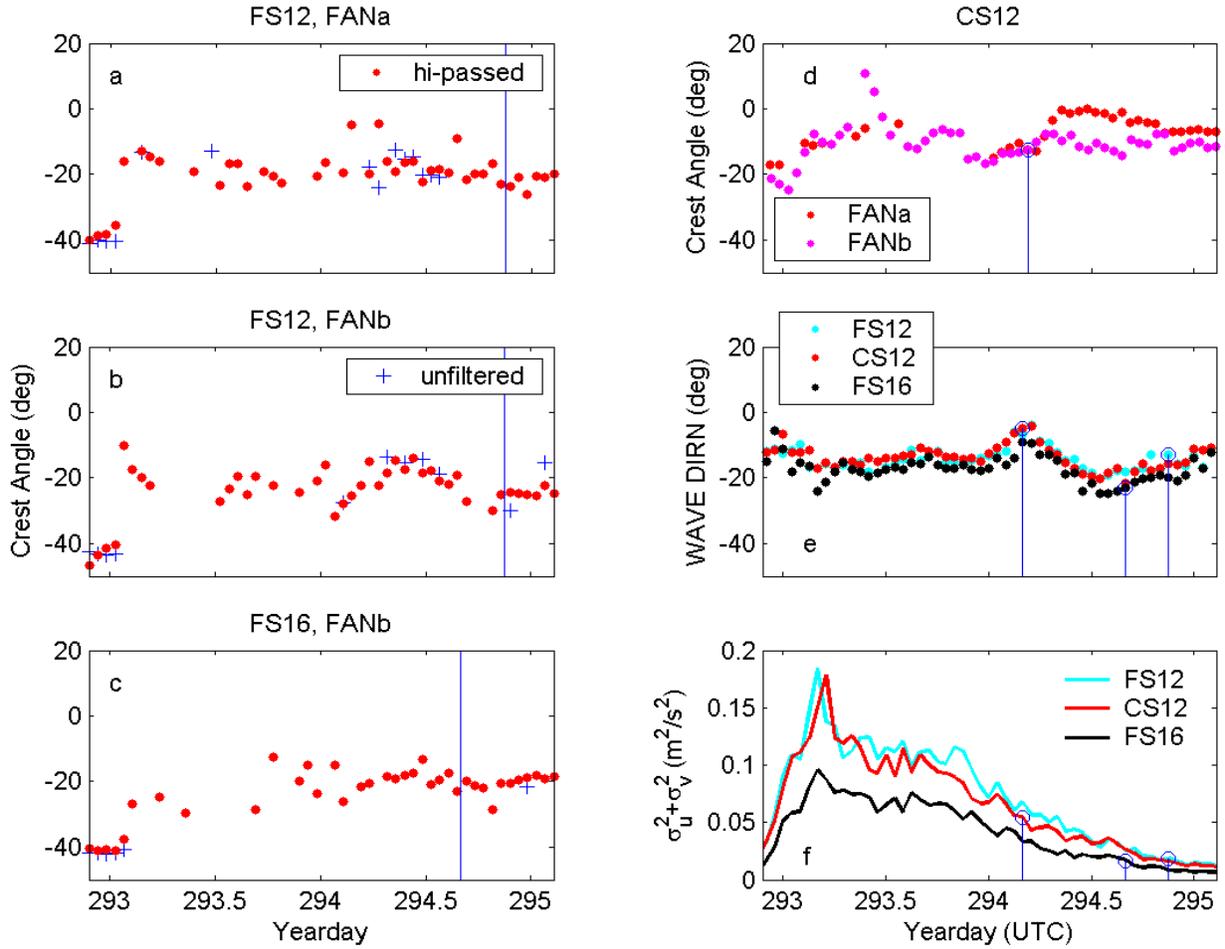


Figure 6. Ripple crest orientation versus wave forcing during the YD293-294 storm event. Panels a through c show the ripple orientations in fine sand obtained using from the unfiltered sonar images (blue crosses) and from the high-pass filtered images (red dots). Panel d shows the orientations in coarse sand. The wave directions and energies are plotted in panels e and f. Vertical blue lines represent the threshold of grain motion at the three sites, as explained in the text.